Relativistic energy-momentum transfer and electromagnetic conservation laws in the interaction of moving charged particles with two-dimensional materials

Zoran L. Mišković,[1,*] Kamran Akbari,[1,†] Silvina Segui,[2,‡] Juana L. Gervasoni,[3,§] and Néstor R. Arista[3]

[1]*Department of Applied Mathematics, University of Waterloo, Waterloo, Ontario, Canada N2L 3G1*

[2]*Centro Atómico Bariloche, Comisión Nacional de Energía Atómica, Avenida Bustillo 9500, 8400 San Carlos de Bariloche, Argentina*

[3]*Centro Atómico Bariloche, Comisión Nacional de Energía Atómica and Instituto Balseiro, Universidad Nacional de Cuyo, Avenida Bustillo 9500, 8400 San Carlos de Bariloche, Argentina*

(Received 9 December 2021; accepted 3 January 2022; published 11 January 2022)

We explore the conservation of energy and momentum by solving Maxwell's equations for a charged particle passing through a single conductive sheet. By using a fully relativistic formulation of the problem, we evaluate the energy and momentum transfer from charged particle to electronic excitations localized in the sheet and to electromagnetic radiation emitted from the sheet in the far-field region. Using a suitable conductivity model for the sheet that can represent graphene or other two-dimensional (2D) material, our theory can elucidate the energy and momentum transfer involving the incident particle, plasmon polariton mode(s) in the 2D material, and the induced transition radiation from it.

DOI: 10.1103/PhysRevB.105.045408

I. INTRODUCTION

Studying interactions of graphene and other two-dimensional (2D) materials with fast charged particles is currently of particular interest for electron energy loss spectroscopy (EELS) in scanning transmission electron microscopy (STEM), which is a powerful technique for probing plasmon excitations in nanostructures for nanophotonic applications in a broad range of frequencies [1,2]. Operating the microscope in the scanning electron microscopy mode enables angle-resolved measurements of the electromagnetic (EM) radiation from the target, giving rise to cathodoluminescence [3,4] or transition radiation (TR) [5,6]. Besides EELS, interactions of fast electrons with 2D materials were also studied in other contexts [7–13], the most notable being the quest for a stable and tunable source of terahertz radiation [14–20].

Studying radiation forces and momenta of light in dielectric media [21] has been a topic of both fundamental interest [22,23] and increasing appeal for applications in nano-optics [24–26] and plasmonics [27,28]. In particular, the concept of the energy velocity [29] was recently used to study electromagnetic energy-momentum flow [30] and angular momentum [27] of light at a boundary between two media supporting surface plasmon polaritons (PPs). On the other hand, there were significant developments in both theoretical modeling and experimental observation of the transfer of electromagnetic energy and momentum in a STEM setting [31,32], with a line of research focusing on forces exerted on plasmonic nanoparticles by a passage of a fast electron beam [33–40]. We have recently developed a fully relativistic theory of the energy loss channels for a fast charged particle interacting with single and multiple layers of graphene under various configurations [41–47]. Our calculations were based on solving Maxwell's equations, where graphene was treated as a planar conductive sheet of zero thickness, containing a 2D electron gas with its dynamic polarization described by an in-plane conductivity σ. Such an approach enabled us to derive analytical expressions for quantities of interest in STEM-EELS experiments, taking the conductivity σ of a general 2D material as an input function [41,47,48], which may be available from empirical models [49] or *ab initio* calculations [47,50–52] covering a broad range frequencies.

While our previous work was mostly concerned with the energy loss channels for particle interactions with 2D materials, there is also an interest in studying the momentum transfer between fast electrons and nanosized targets [33–40]. Having in mind recent achievements in using electron diffraction-based techniques to probe suspended van der Waals heterostructures in STEM [53], it is interesting to explore the mechanisms of momentum transfer from a fast charged particle to a 2D material via a *purely* EM interaction [54]. In that respect, we study in this work the conservation equations for both energy and momentum in a system, consisting of three subsystems: an external moving charge, electronic excitations in a 2D material, and the EM fields radiated in the far-field region. In doing so, we appeal to a probabilistic interpretation of the processes involved [55–57] and obtain analytical expressions for three functions of the parallel wavevector $\mathbf{k}$ and angular frequency ω, which we

*zmiskovi@uwaterloo.ca; also at Waterloo Institute for Nanotechnology, University of Waterloo, Waterloo, Ontario, Canada N2L 3G1.

†kakbari@uwaterloo.ca

‡segui@cab.cnea.gov.ar; also at Consejo Nacional de Investigaciones Científicas y Técnicas of Argentina (CONICET).

§Also at Consejo Nacional de Investigaciones Científicas y Técnicas of Argentina (CONICET).

 ©2022 American Physical Society

call $F_{\rm ext}$, $F_{\rm ohm}$, and $F_{\rm rad}$ and interpret as joint (probability) densities, making it possible to evaluate the first and higher (marginal) moments of changes in the parallel and perpendicular momenta, as well as the energy, that occur within each subsystem during the passage of the charged particle.

Our formalism also opens access to evaluating the forces that act on both the incident particle and the target as a whole, which could be observed in STEM. An important difference from the previous work on plasmonic nanoparticles [33,34,39,40] and the planar boundary of a solid target [37,38] is that in our case the incident particle passes through a 2D target. Representing a 2D (or atomically thin) material as an infinitesimally thin, continuous sheet enables its efficient inclusion in the framework of classical Maxwell equations via standard boundary conditions, augmented by a constitutive relation in the form of an in-plane Ohm law [58,59]. While this is certainly advantageous for modeling of the quantities that are accessible in STEM-EELS experiments [49], the use of a Dirac delta "function" to represent a 2D material can be problematic when attempting to calculate the energy and momentum that are associated with electron excitations localized in such a material. We tackle this problem with special care in this work, and provide a solution that is consistent with the conservation equations for the entire system. The resulting expressions for the momentum exchange between its subsystems can shed light not only on the forces acting on the external particle and the target, but also on the possibility to use the energy and direction of that particle to achieve directionality in launching PPs in 2D materials [12,13,45,60]. Moreover, our results may be of interest for recent advances in electron detection techniques, which allow performing rapid scanning-diffraction experiments with high sensitivity and high dynamic range, giving rise to a form of four-dimensional momentum-resolved imaging of nanomaterials [61].

In the theoretical section, we first use the Poynting theorem to rederive the relations pertaining to the energy conservation invoked in our previous work, which is followed by the use of a momentum conservation equation employing the Maxwell stress tensor to derive expressions for the momentum transfer between different subsystems. While the main body of the article deals explicitly with normal incidence of a charged particle on a 2D material described by a scalar longitudinal conductivity, we outline in the Appendix all the necessary generalizations to the case of oblique incidence and a 2D material described by tensorial in-plane conductivity.

We use the Gaussian units of electrodynamics [62].

II. THEORETICAL MODEL

For the sake of self-containment and consistency with conservation equations that are studied later in this section, several prior results will be rederived using a more direct formulation than in, e.g., Ref. [41]. We consider an infinitely large and infinitesimally thin planar conductive sheet, placed in vacuum and lying in the $z = 0$ plane of a Cartesian coordinate system with $\mathbf{R} = \{\mathbf{r}, z\}$, where $\mathbf{r} = \{x, y\}$ (see Fig. 1). We assume that a fast pointlike particle with charge Ze (where $Z = -1$ for an incident electron and $Z > 0$ for an incident ion) moves along the z axis with constant velocity $\mathbf{v}$ and passes through the sheet at time $t = 0$, so that its charge

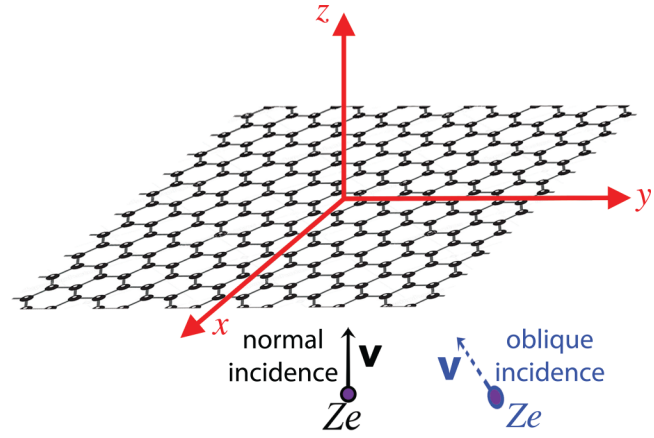

FIG. 1. Schematic diagram shows a particle of charge Ze moving with the velocity $\mathbf{v}$ and passing through a single layer of graphene, which occupies the (x, y) plane. The case of normal incidence is discussed in the main text, while the more general case of oblique incidence is discussed in the Appendix.

density is $\rho_{\rm ext}(\mathbf{R}, t) = Ze\,\delta(\mathbf{r})\,\delta(z - vt)$ and current density is $\mathbf{J}_{\rm ext}(\mathbf{R}, t) = \hat{\mathbf{z}}\,v\rho_{\rm ext}(\mathbf{R}, t)$, where $v = \|\mathbf{v}\|$ is its speed and $\hat{\mathbf{z}}$ is the unit vector in the direction of the z axis. Maxwell's equations are easily tackled for this problem by assuming a translational invariance of the sheet and performing Fourier transform (FT) with respect to the in-plane coordinates ($\mathbf{r} \to \mathbf{k} = \{k_x, k_y\}$) and a FT with respect to time ($t \to \omega$). We use a tilde to indicate a Fourier-transformed function, so that, for example, the charge current density of the external particle is written as

$$\mathbf{J}_{\rm ext}(\mathbf{R}, t) = \iint \frac{d^2\mathbf{k}}{(2\pi)^2} \int_{-\infty}^{\infty} \frac{d\omega}{2\pi}\, \mathrm{e}^{i\mathbf{k}\cdot\mathbf{r} - i\omega t}\, \widetilde{\mathbf{J}}_{\rm ext}(\mathbf{k}, z, \omega). \quad (1)$$

If we decompose the electric and magnetic fields generated by the external charged particle into their parallel and perpendicular components, $\mathbf{E}_{\rm ext} = \mathbf{E}^{\parallel}_{\rm ext} + \hat{\mathbf{z}}\,E^{\perp}_{\rm ext}$ and $\mathbf{B}_{\rm ext} = \mathbf{B}^{\parallel}_{\rm ext} + \hat{\mathbf{z}}\,B^{\perp}_{\rm ext}$, we obtain in the FT domain [41]

$$\begin{aligned}
\widetilde{\mathbf{E}}^{\parallel}_{\rm ext}(\mathbf{k}, z, \omega) &= -i\mathbf{k}\frac{Ze}{v}A\,\mathrm{e}^{iz\frac{\omega}{v}},\\
\widetilde{E}^{\perp}_{\rm ext}(k, z, \omega) &= -iZeA\omega\left(\frac{1}{v^2} - \frac{1}{c^2}\right)\mathrm{e}^{iz\frac{\omega}{v}},\\
\widetilde{\mathbf{B}}^{\parallel}_{\rm ext}(\mathbf{k}, z, \omega) &= -i(\hat{\mathbf{z}} \times \mathbf{k})\frac{Ze}{c}A\,\mathrm{e}^{iz\frac{\omega}{v}},
\end{aligned} \quad (2)$$

and $\widetilde{B}^{\perp}_{\rm ext}(\mathbf{k}, z, \omega) = 0$, with A being an auxiliary amplitude, defined by

$$A(k, \omega) = \frac{4\pi}{\frac{\omega^2}{v^2} - \frac{\omega^2}{c^2} + k^2}, \quad (3)$$

where $k = \|\mathbf{k}\| = \sqrt{k_x^2 + k_y^2}$.

We describe dynamic polarization of the sheet by using a continuous model for its in-plane conductivity σ. Assuming that the sheet is isotropic in the (x, y) plane, it suffices to use a scalar conductivity function $\sigma(k, \omega)$ to describe longitudinal fields because no transverse fields are induced in the case of normal incidence of the external charged particle, as shown in Ref. [45]. A crucial step in solving Maxwell's

equations for the electric and magnetic fields, $\mathbf{E}_{\rm ind}$ and $\mathbf{B}_{\rm ind}$, which are generated by the charge current density induced in the sheet, $\widetilde{\mathbf{J}}_{\rm ind}(\mathbf{k},z,\omega)=\delta(z)\,\widetilde{\mathbf{J}}_{2D}(\mathbf{k},\omega)$, is the use of an in-plane Ohm law to express the in-plane current density in that sheet as $\widetilde{\mathbf{J}}_{2D}(\mathbf{k},\omega)=\sigma(k,\omega)\,\widetilde{\mathbf{E}}_{\parallel}(\mathbf{k},0,\omega)$. Here, $\widetilde{\mathbf{E}}_{\parallel}(\mathbf{k},0,\omega)$ is the FT of the parallel component of the total electric field, $\mathbf{E}=\mathbf{E}_{\rm ext}+\mathbf{E}_{\rm ind}$, evaluated at $z=0$, which we may simply call the in-plane electric field [41]. By expressing the standard boundary condition [62] for the parallel component of the total magnetic field, $\widetilde{\mathbf{H}}_{\parallel}=\widetilde{\mathbf{B}}_{\parallel}=\widetilde{\mathbf{B}}^{\parallel}_{\rm ext}+\widetilde{\mathbf{B}}^{\parallel}_{\rm ind}$ at $z=0$ in terms of $\widetilde{\mathbf{J}}_{2D}(\mathbf{k},\omega)$ [or, equivalently, expressing the boundary condition for normal component of the total electric field $\widetilde{E}_{\perp}=\widetilde{E}^{\perp}_{\rm ext}+\widetilde{E}^{\perp}_{\rm ind}$ at $z=0$ in terms of the associated induced 2D charge density per unit area in the sheet, $\widetilde{\rho}_{2D}(\mathbf{k},\omega)=\frac{1}{\omega}\mathbf{k}\cdot\widetilde{\mathbf{J}}_{2D}(\mathbf{k},\omega)$, which follows from the in-plane continuity equation], we find a self-consistent solution for the in-plane electric field as [41]

$$\widetilde{\mathbf{E}}_{\parallel}(\mathbf{k},0,\omega)=-i\mathbf{k}\frac{Ze}{v}\frac{A(k,\omega)}{\epsilon(k,\omega)}. \tag{4}$$

Here, we introduced $\epsilon(k,\omega)=1+\frac{2\pi}{\omega}q(k,\omega)\,\sigma(k,\omega)$ as an effective 2D longitudinal dielectric permittivity of the sheet, with

$$q(k,\omega)=\begin{cases}\mathrm{sign}(\omega)\sqrt{\left(\frac{\omega}{c}\right)^2-k^2}, & |\omega|>ck\\ i\sqrt{k^2-\left(\frac{\omega}{c}\right)^2}, & |\omega|<ck,\end{cases} \tag{5}$$

where EM is the wavenumber in the direction perpendicular to the sheet. The expression in Eq. (4) enables us to obtain the induced electric and magnetic fields in the regions outside the sheet, which, when decomposed into the parallel and perpendicular components according to $\mathbf{E}_{\rm ind}=\mathbf{E}^{\parallel}_{\rm ind}+\hat{\mathbf{z}}\,E^{\perp}_{\rm ind}$ and $\mathbf{B}_{\rm ind}=\mathbf{B}^{\parallel}_{\rm ind}+\hat{\mathbf{z}}\,B^{\perp}_{\rm ind}$, may be written in the FT domain as [41]

$$\begin{aligned}\widetilde{\mathbf{E}}^{\parallel}_{\rm ind}(\mathbf{k},z,\omega)&=i2\pi\mathbf{k}\frac{Ze}{v}A\frac{q}{\omega}\frac{\sigma}{\epsilon}\,\mathrm{e}^{iq|z|},\\ \widetilde{E}^{\perp}_{\rm ind}(k,z,\omega)&=-i2\pi\frac{Ze}{v}A\frac{k^2}{\omega}\frac{\sigma}{\epsilon}\,\mathrm{e}^{iq|z|}\,\mathrm{sign}(z),\\ \widetilde{\mathbf{B}}^{\parallel}_{\rm ind}(\mathbf{k},z,\omega)&=i2\pi(\hat{\mathbf{z}}\times\mathbf{k})\frac{Ze}{c}\frac{A}{v}\frac{\sigma}{\epsilon}\,\mathrm{e}^{iq|z|}\,\mathrm{sign}(z),\end{aligned} \tag{6}$$

and $\widetilde{B}^{\perp}_{\rm ind}(\mathbf{k},z,\omega)=0$, where $\mathrm{sign}(\cdot)$ is the signum function, defined as $\mathrm{sign}(z)=\pm1$ for $z\gtrless0$. To keep displayed equations compact, the functions $A(k,\omega)$, $q(k,\omega)$, $\sigma(k,\omega)$, and $\epsilon(k,\omega)$ are hereafter written without showing their explicit dependencies on the variables k and ω.

A. Energy conservation

In Ref. [41], we showed that the total energy lost by the external charged particle upon passing through the sheet goes into the energy deposited in that sheet in the form of electronic excitations, including any PP modes, which we call summarily the Ohmic loss, and the energy that is emitted in the far-field region in the form of TR. Here, we use the Poynting theorem to show that those energy loss channels are balanced by integrating the conservation of energy equation [62,63],

$$\frac{dW}{dt}+\frac{dU_{\rm EM}}{dt}+\oiint_{\partial V}\mathbf{S}\cdot\hat{\mathbf{n}}\,dA=0, \tag{7}$$

where $\frac{dW}{dt}=\iiint_V\mathbf{E}\cdot\mathbf{J}\,dV$ is the rate at which work is done on all charges in some volume V by the EM fields, $U_{\rm EM}=\frac{1}{8\pi}\iiint_V(\mathbf{E}^2+\mathbf{B}^2)\,dV$ is the total energy stored in the EM fields in that volume, and the third term is the flux of the Poynting vector $\mathbf{S}=\frac{c}{4\pi}\mathbf{E}\times\mathbf{B}$ through the boundary ∂V of that volume, with $\hat{\mathbf{n}}$ being its outward-pointing unit normal vector. We take V to be the region between two planes, $z=\pm d$, which are parallel to the sheet and are placed a distance $d\to\infty$ from it, so that $\hat{\mathbf{n}}=\pm\hat{\mathbf{z}}$ when $z\gtrless0$.

Upon integrating each term in Eq. (7) over time $t\in(-\infty,\infty)$, we can switch to the FT domain by invoking the pertinent symmetry properties, e.g., $\widetilde{\mathbf{E}}(-\mathbf{k},z,-\omega)=\widetilde{\mathbf{E}}^*(\mathbf{k},z,\omega)$, where the symbol $*$ indicates a complex conjugate. Accordingly, we obtain from the first term in Eq. (7)

$$W=\frac{1}{4\pi^3}\int_0^\infty d\omega\iint d^2\mathbf{k}\int_{-d}^{d}dz\times\mathrm{Re}[\widetilde{\mathbf{E}}(\mathbf{k},z,\omega)\cdot\widetilde{\mathbf{J}}^*(\mathbf{k},z,\omega)], \tag{8}$$

with Re used hereafter to indicate the "real part" of an expression written in the FT domain. By decomposing the total current density into external and induced parts, $\widetilde{\mathbf{J}}=\widetilde{\mathbf{J}}_{\rm ext}+\widetilde{\mathbf{J}}_{\rm ind}$, we can write $W=W_{\rm ext}+W_{\rm ohm}$, where the total energy lost by the external charged particle may be evaluated as the first moment with respect to frequency,

$$W_{\rm ext}=-\int_0^\infty d\omega\,\omega\iint d^2\mathbf{k}\,F_{\rm ext}(k,\omega)<0, \tag{9}$$

with the joint density for transferring the momentum $\hbar\mathbf{k}$ and energy $\hbar\omega$ to the sheet given by [41]

$$\begin{aligned}F_{\rm ext}(k,\omega)&=\frac{1}{4\pi^3\omega}\int_{-\infty}^{\infty}dz\,\mathrm{Re}[\widetilde{\mathbf{E}}_{\rm ind}(\mathbf{k},z,\omega)\cdot\widetilde{\mathbf{J}}^*_{\rm ext}(\mathbf{k},z,\omega)]\\&=\frac{(Ze)^2}{v^2}\frac{A^2}{4\pi^3}\frac{k^2}{\omega}\mathrm{Re}\left[\frac{\sigma}{\epsilon}\right].\end{aligned} \tag{10}$$

The energy that remains localized in the sheet in the form of electronic excitations is obtained from Eq. (8) as

$$W_{\rm ohm}=\int_0^\infty d\omega\,\omega\iint d^2\mathbf{k}\,F_{\rm ohm}(k,\omega)>0, \tag{11}$$

with the corresponding joint density given by

$$\begin{aligned}F_{\rm ohm}(k,\omega)&=\frac{1}{4\pi^3\omega}\int_{-\infty}^{\infty}dz\,\mathrm{Re}[\widetilde{\mathbf{E}}(\mathbf{k},z,\omega)\cdot\widetilde{\mathbf{J}}^*_{\rm ind}(\mathbf{k},z,\omega)]\\&=\frac{\mathrm{Re}[\sigma]}{4\pi^3\omega}\widetilde{\mathbf{E}}_{\parallel}(\mathbf{k},0,\omega)\cdot\widetilde{\mathbf{E}}^*_{\parallel}(\mathbf{k},0,\omega).\end{aligned} \tag{12}$$

Using Eq. (4) for the in-plane electric field, we confirm that Eq. (12) gives the result quoted in Eq. (34) of Ref. [41].

Upon integrating the second term in Eq. (7) over time, we obtain $U_{\rm EM}(\infty)-U_{\rm EM}(-\infty)$, which is zero because the fraction of the EM energy $U_{\rm EM}$ associated with the external charged particle is constant in time, whereas the fraction of $U_{\rm EM}$ pertaining to the induced EM fields may be assumed to be zero for $t\to-\infty$ and to vanish when $t\to\infty$ if we

allow for small losses in the sheet that may be described by adding damping terms in its conductivity that give finite $\mathrm{Re}[\sigma(k,\omega)] > 0$. On the other hand, by integrating the third term in Eq. (7) over time, we can express the energy carried away in the far field in the form of TR as

$$W_{\mathrm{rad}} = \int_{-\infty}^{\infty} dt \oiint_{\partial V} \mathbf{S}\cdot\hat{\mathbf{n}}\, dA$$
$$= \frac{c}{(2\pi)^4}\int_0^{\infty} d\omega \iint d^2\mathbf{k}\,\mathrm{Re}\{\hat{\mathbf{z}}\cdot[\widetilde{\mathbf{E}}(\mathbf{k},d,\omega) \times \widetilde{\mathbf{B}}^*(\mathbf{k},d,\omega) - \widetilde{\mathbf{E}}(\mathbf{k},-d,\omega)\times\widetilde{\mathbf{B}}^*(\mathbf{k},-d,\omega)]\}, \quad (13)$$

where the total electric and magnetic fields should be decomposed into their external and induced components. The resulting interference terms between those two field components vanish because they contain factors $\exp[\pm id(\frac{\omega}{v}\pm q)]$, which rapidly oscillate when $d\to\infty$. Moreover, the contribution to the integral in Eq. (13) from the external fields vanishes because the associated Poynting vector is constant along the z axis. Thus, the only contribution to Eq. (13) comes from the Poynting vector associated with the induced EM fields, which may be written in the FT domain as

$$\widetilde{\mathbf{S}}_{\mathrm{ind}}(\mathbf{k},z,\omega) = \frac{c}{4\pi}\widetilde{\mathbf{E}}_{\mathrm{ind}}(\mathbf{k},z,\omega)\times\widetilde{\mathbf{B}}^*_{\mathrm{ind}}(\mathbf{k},z,\omega)$$
$$= [\mathbf{k}+\hat{\mathbf{z}}\,q\,\mathrm{sign}(z)]\frac{\pi}{\omega}\left(\frac{Ze}{v}Ak\right)^2\left|\frac{\sigma}{\epsilon}\right|^2. \quad (14)$$

Given that $\widetilde{\mathbf{S}}_{\mathrm{ind}}(\mathbf{k},z,\omega)$ exhibits a finite jump at $z=0$ and is otherwise constant in the regions above and below the sheet, we may finally express the radiation energy loss as

$$W_{\mathrm{rad}} = \int_0^{\infty} d\omega\,\omega \iint d^2\mathbf{k}\,F_{\mathrm{rad}}(k,\omega) > 0, \quad (15)$$

where the corresponding joint density is obtained from the fluxes of the induced Poynting vector through the planes $z=0^{\pm}$, which envelop the sheet tightly, as

$$F_{\mathrm{rad}}(k,\omega) = \frac{1}{4\pi^3\omega}\mathrm{Re}\{\hat{\mathbf{z}}\cdot[\widetilde{\mathbf{S}}_{\mathrm{ind}}(\mathbf{k},0^+,\omega) - \widetilde{\mathbf{S}}_{\mathrm{ind}}(\mathbf{k},0^-,\omega)]\}. \quad (16)$$

Using here $\widetilde{\mathbf{S}}_{\mathrm{ind}}$ from Eq. (14) yields an expression for F_{rad}, which reproduces Eq. (35) of Ref. [41].

Finally, referring to Eqs. (9), (11), and (15), along with the corresponding definitions of the joint densities in Eqs. (10), (12), and (16), we have confirmed that the Poynting theorem, Eq. (7), upholds the energy conservation as $W_{\mathrm{ext}} + W_{\mathrm{ohm}} + W_{\mathrm{rad}} = 0$ or, equivalently, as $F_{\mathrm{ext}} = F_{\mathrm{ohm}} + F_{\mathrm{rad}}$. We note that expressions for F_{ohm} and F_{rad} are readily derived from the expression for F_{ext} by expanding the factor $\mathrm{Re}[\frac{\sigma}{\epsilon}]$ in Eq. (10) according to

$$\mathrm{Re}\left[\frac{\sigma}{\epsilon}\right] = \frac{\mathrm{Re}[\sigma]}{|\epsilon|^2} + 2\pi\frac{q}{\omega}\left|\frac{\sigma}{\epsilon}\right|^2 H(|\omega|-ck), \quad (17)$$

where $H(\cdot)$ is a Heaviside unit step function, which results from the definition of q in Eq. (5). As a consequence, the radiative probability density, F_{rad}, which results from the second term in the above equation, is only nonzero above the light cone, $|\omega| > ck$. On the other hand, when the 2D material supports a collective mode, such as a PP with negligible damping, $\mathrm{Re}[\sigma]\to 0^+$, then the first term in the above equation gives rise to Ohmic probability density F_{ohm} featuring a Dirac delta peaked at its dispersion relation, say, $\omega = \omega_p(\mathbf{k})$, which is located below the light cone, $|\omega| < ck$, and it additionally enforces an energy-momentum relation pertaining to that mode. In that case, our designation "Ohmic" for the function F_{ohm} should be more appropriately replaced by a designation "plasmonic" [44].

B. Momentum conservation

While the expressions obtained in the preceding section for energy conservation are not new, we now explore conservation of momentum by considering the equation [63]

$$\frac{d\mathbf{p}}{dt} + \frac{1}{c^2}\frac{d}{dt}\iiint_V \mathbf{S}\,dV - \oiint_{\partial V}\overleftrightarrow{\mathbf{T}}\cdot\hat{\mathbf{n}}\,dA = 0, \quad (18)$$

where the first term is the time-dependent Lorentz force on all charges in the system,

$$\frac{d\mathbf{p}}{dt} = \iiint_V\left[\rho(\mathbf{R},t)\mathbf{E}(\mathbf{R},t) + \frac{1}{c}\mathbf{J}(\mathbf{R},t)\times\mathbf{B}(\mathbf{R},t)\right]dV, \quad (19)$$

with $\rho = \rho_{\mathrm{ext}} + \rho_{\mathrm{ind}}$ being the total charge density, the second term the rate of change of the total momentum of the EM fields in the volume V, and the third term the flux of the Maxwell stress tensor [62],

$$\overleftrightarrow{\mathbf{T}}(\mathbf{R},t) = \frac{1}{4\pi}\left[\mathbf{EE}+\mathbf{BB}-\frac{1}{2}(\mathbf{E}\cdot\mathbf{E}+\mathbf{B}\cdot\mathbf{B})\overleftrightarrow{I}\right], \quad (20)$$

through the boundary ∂V of that volume with $\hat{\mathbf{n}}$ being its outward-pointing unit normal vector.

As in the preceding section, we use the same volume V, integrate Eq. (18) over time $t\in(-\infty,\infty)$, and switch to the FT domain. Accordingly, the first term gives us the total momentum imparted on all charges in V by the EM fields, which can be expressed upon decomposing ρ, $\mathbf{J}$, $\mathbf{E}$, and $\mathbf{B}$ into their respective external and induced parts as $\mathbf{p} = \mathbf{p}_{\mathrm{ext}} + \mathbf{p}_{\mathrm{ohm}}$, where

$$\mathbf{p}_{\mathrm{ext}} = \frac{1}{4\pi^3}\int_0^{\infty} d\omega \iint d^2\mathbf{k}\int_{-d}^{d} dz\,\mathrm{Re}\left[\widetilde{\rho}_{\mathrm{ext}}(\mathbf{k},z,\omega)\widetilde{\mathbf{E}}^*_{\mathrm{ind}}(\mathbf{k},z,\omega) + \frac{1}{c}\widetilde{\mathbf{J}}_{\mathrm{ext}}(\mathbf{k},z,\omega)\times\widetilde{\mathbf{B}}^*_{\mathrm{ind}}(\mathbf{k},z,\omega)\right] \quad (21)$$

is the total change of momentum of the external charged particle, and

$$\mathbf{p}_{\mathrm{ohm}} = \frac{1}{4\pi^3}\int_0^{\infty} d\omega \iint d^2\mathbf{k}\int_{-d}^{d} dz\,\mathrm{Re}\left[\widetilde{\rho}_{\mathrm{ind}}(\mathbf{k},z,\omega)\widetilde{\mathbf{E}}^*(\mathbf{k},z,\omega) + \frac{1}{c}\widetilde{\mathbf{J}}_{\mathrm{ind}}(\mathbf{k},z,\omega)\times\widetilde{\mathbf{B}}^*(\mathbf{k},z,\omega)\right] \quad (22)$$

is the total momentum transferred to the conductive sheet. Taking the limit $d \to \infty$ in Eq. (21), calculations show that the momentum change of the external charged particle may be expressed as the first moment as

$$\mathbf{p}_{\rm ext} = -\int_0^\infty d\omega \iint d^2\mathbf{k} \left(\mathbf{k} + \hat{\mathbf{z}}\frac{\omega}{v}\right) F_{\rm ext}(k,\omega), \tag{23}$$

where $F_{\rm ext}$ is given in Eq. (10) and is consistently interpreted as the joint density that the external particle changes its momentum by $\hbar\mathbf{k}$ in the parallel direction and by the amount $\frac{\hbar\omega}{v}$ in the perpendicular direction with respect to the sheet. Clearly, referring to Eq. (9), we may conclude from Eq. (23) that $W_{\rm ext} = \mathbf{v}\cdot\mathbf{p}_{\rm ext}$, as expected in our approximation of negligible recoil for the external particle's trajectory.

Evaluation of the integrals in Eq. (22) for the momentum transferred to the sheet requires more care because both the induced current density $\widetilde{\mathbf{J}}_{\rm ind}(\mathbf{k},z,\omega) = \delta(z)\,\widetilde{\mathbf{J}}_{\rm 2D}(\mathbf{k},\omega) = \delta(z)\,\sigma(k,\omega)\,\widetilde{\mathbf{E}}_\parallel(\mathbf{k},0,\omega)$ and the corresponding induced charge density, $\widetilde{\rho}_{\rm ind}(\mathbf{k},z,\omega) = \delta(z)\,\widetilde{\rho}_{\rm 2D}(\mathbf{k},\omega) = \delta(z)\,\frac{\sigma(k,\omega)}{\omega}\,\mathbf{k}\cdot\widetilde{\mathbf{E}}_\parallel(\mathbf{k},0,\omega)$ include a Dirac delta $\delta(z)$. Namely, while the parallel components of vector fields in the integrand in Eq. (22) are continuous functions of z, a problem arises with their perpendicular components, because both $\widetilde{E}_\perp(\mathbf{k},z,\omega)$ and $\widetilde{\mathbf{B}}_\parallel(\mathbf{k},z,\omega)$ exhibit jump discontinuities at $z=0$. Postponing the definition of the values of those fields at $z=0$ until the next paragraph, we invoke a formal sifting property of $\delta(z)$ and obtain from Eq. (22)

$$\begin{aligned}\mathbf{p}_{\rm ohm} = \frac{1}{4\pi^3}\int_0^\infty d\omega \iint d^2\mathbf{k} \\ \times {\rm Re}\Bigg[\frac{\sigma}{\omega}\big(\mathbf{k}\cdot\widetilde{\mathbf{E}}_\parallel(\mathbf{k},0,\omega)\big)\widetilde{\mathbf{E}}^*(\mathbf{k},0,\omega) \\ + \frac{\sigma}{c}\,\widetilde{\mathbf{E}}_\parallel(\mathbf{k},0,\omega)\times\widetilde{\mathbf{B}}^*_\parallel(\mathbf{k},0,\omega)\Bigg],\end{aligned} \tag{24}$$

where we recalled that $\widetilde{B}_\perp(\mathbf{k},z,\omega) = 0$ for all z, including $z=0$. It is therefore convenient to decompose the momentum transferred to the sheet into parallel and perpendicular components, $\mathbf{p}_{\rm ohm} = \mathbf{p}^\parallel_{\rm ohm} + \hat{\mathbf{z}}\,p^\perp_{\rm ohm}$. With $\widetilde{\mathbf{E}}_\parallel(\mathbf{k},0,\omega)$ given in Eq. (4), the parallel component is obtained from the first term inside the brackets in Eq. (24) as

$$\begin{aligned}\mathbf{p}^\parallel_{\rm ohm} &= \frac{1}{4\pi^3}\int_0^\infty d\omega \iint d^2\mathbf{k} \\ &\quad\times {\rm Re}\Bigg[\frac{\sigma}{\omega}\big(\mathbf{k}\cdot\widetilde{\mathbf{E}}_\parallel(\mathbf{k},0,\omega)\big)\widetilde{\mathbf{E}}^*_\parallel(\mathbf{k},0,\omega)\Bigg] \\ &= \int_0^\infty d\omega \iint d^2\mathbf{k}\,\mathbf{k}\,F_{\rm ohm}(k,\omega),\end{aligned} \tag{25}$$

where $F_{\rm ohm}(k,\omega)$ is the joint density for Ohmic energy loss discussed in Eq. (12).

For the perpendicular component of the momentum transferred to the sheet, we need to define the value of the perpendicular component of the total electric field $\widetilde{E}_\perp$ at $z=0$ and the value of the tangential component of the total magnetic field $\widetilde{\mathbf{B}}_\parallel$ at $z=0$. To do so, we invoke an argument made elsewhere [64–66] that those values should be defined as arithmetic means of the values of the respective fields at $z=0^+$ and $z=0^-$,

$$\widetilde{E}_\perp(\mathbf{k},0,\omega) = \frac{1}{2}[\widetilde{E}_\perp(\mathbf{k},0^+,\omega) + \widetilde{E}_\perp(\mathbf{k},0^-,\omega)], \tag{26}$$

$$\widetilde{\mathbf{B}}_\parallel(\mathbf{k},0,\omega) = \frac{1}{2}[\widetilde{\mathbf{B}}_\parallel(\mathbf{k},0^+,\omega) + \widetilde{\mathbf{B}}_\parallel(\mathbf{k},0^-,\omega)]. \tag{27}$$

Therefore, we obtain $\widetilde{E}_\perp(\mathbf{k},0,\omega) = \widetilde{E}^\perp_{\rm ext}(\mathbf{k},0,\omega)$ and $\widetilde{\mathbf{B}}_\parallel(\mathbf{k},0,\omega) = \widetilde{\mathbf{B}}^\parallel_{\rm ext}(\mathbf{k},0,\omega)$, which could be incorporated in the expressions for induced fields in Eq. (6) by extending the definition of the signum function to $z=0$, so that ${\rm sign}(0)=0$. Incorporating this result in Eq. (24) gives for the perpendicular component of the momentum transferred to the sheet

$$\begin{aligned}p^\perp_{\rm ohm} &= \frac{1}{4\pi^3}\int_0^\infty d\omega \iint d^2\mathbf{k} \\ &\quad\times {\rm Re}\Bigg[\frac{\sigma}{\omega}\big(\mathbf{k}\cdot\widetilde{\mathbf{E}}_\parallel(\mathbf{k},0,\omega)\big)\widetilde{E}^{\perp *}_{\rm ext}(\mathbf{k},0,\omega) \\ &\quad + \frac{\sigma}{c}\,\hat{\mathbf{z}}\cdot\big(\widetilde{\mathbf{E}}_\parallel(\mathbf{k},0,\omega)\times\widetilde{\mathbf{B}}^{\parallel *}_{\rm ext}(\mathbf{k},0,\omega)\big)\Bigg] \\ &= \int_0^\infty d\omega \iint d^2\mathbf{k}\,\frac{\omega}{v}\,F_{\rm ext}(k,\omega),\end{aligned} \tag{28}$$

where $F_{\rm ext}(k,\omega)$ is the joint density given in Eq. (10).

Invoking the relation $F_{\rm ext} = F_{\rm ohm} + F_{\rm rad}$ deduced in the preceding section and using Eqs. (23), (25), and (28), it is remarkable that the total momentum imparted on all charges in the system by the EM fields adds up to the negative of the first moment of parallel momentum carried away by radiation in the far field,

$$\begin{aligned}\mathbf{p} &= \mathbf{p}_{\rm ext} + (\mathbf{p}^\parallel_{\rm ohm} + \hat{\mathbf{z}}\,p^\perp_{\rm ohm}) \\ &= -\int_0^\infty d\omega \iint d^2\mathbf{k}\,\mathbf{k}\,F_{\rm rad}(k,\omega),\end{aligned} \tag{29}$$

where $F_{\rm rad}(k,\omega)$ is the joint density for TR discussed in Eq. (16).

To verify the conservation of momentum, we remark that integration over time of the second term in Eq. (18) gives zero using the same arguments as for the second term in Eq. (7). Thus, we focus on the third term in Eq. (18) and define the momentum $\mathbf{p}_{\rm rad}$ carried by the EM fields in the far-field region as the negative of the time integral of the flux of the Maxwell stress tensor $\overleftrightarrow{\mathbf{T}}$ through the planes $z = \pm d$ with $d \to \infty$. Letting $p_{{\rm rad},j}$ be the jth Cartesian component of that momentum, so that $\mathbf{p}^\parallel_{\rm rad} = \hat{\mathbf{x}}\,p_{{\rm rad},x} + \hat{\mathbf{y}}\,p_{{\rm rad},y}$ in the parallel direction and $p^\perp_{\rm rad} \equiv p_{{\rm rad},z}$ in the perpendicular direction, we can write for $j = x,y,z$

$$\begin{aligned}p_{{\rm rad},j} &= -\int_{-\infty}^\infty dt \oiint_{\partial V} \hat{\boldsymbol{\jmath}}\cdot\overleftrightarrow{\mathbf{T}}\cdot\hat{\mathbf{n}}\,dA \\ &= -\frac{1}{4\pi^3}\int_0^\infty d\omega \iint d^2\mathbf{k} \\ &\quad\times {\rm Re}[\widetilde{T}_{jz}(\mathbf{k},d,\omega) - \widetilde{T}_{jz}(\mathbf{k},-d,\omega)],\end{aligned} \tag{30}$$

where $\hat{\boldsymbol{\jmath}}$ is the unit vector along the jth axis, while the Cartesian components of the tensor $\overleftrightarrow{\mathbf{T}}$ are defined in the FT

domain as

$$\widetilde{T}_{j\ell}(\mathbf{k}, z, \omega) = \frac{1}{4\pi}\left[\widetilde{E}_j\widetilde{E}^*_\ell + \widetilde{B}_j\widetilde{B}^*_\ell - \frac{1}{2}(\widetilde{\mathbf{E}}\cdot\widetilde{\mathbf{E}}^* + \widetilde{\mathbf{B}}\cdot\widetilde{\mathbf{B}}^*)\delta_{j\ell}\right]. \tag{31}$$

As with the flux of the Poynting vector in the preceding section, we note that the total electric and magnetic fields in this equation should be decomposed into their external and induced parts and that the resulting interference terms vanish because of the fast oscillations in the factors $\exp[\pm id(\frac{\omega}{v} \pm q)]$ when $d \to \infty$. Moreover, because the tensor components associated with the external particle do not depend on z, it is only the jump at $z = 0$ in the stress tensor components associated with the induced fields that ultimately gives rise to a nonzero net flux through the planes $z = \pm d$. For the parallel direction, we obtain from Eqs. (30) and (31), along with Eq. (6),

$$\begin{aligned}\mathbf{p}^{\parallel}_{\text{rad}} &= -\frac{1}{16\pi^4}\int_0^\infty d\omega \iint d^2\mathbf{k}\,\text{Re}\big[\widetilde{\mathbf{E}}^{\parallel}_{\text{ind}}(\mathbf{k}, d, \omega)\widetilde{E}^{\perp *}_{\text{ind}}(\mathbf{k}, d, \omega) - \widetilde{\mathbf{E}}^{\parallel}_{\text{ind}}(\mathbf{k}, -d, \omega)\widetilde{E}^{\perp *}_{\text{ind}}(\mathbf{k}, -d, \omega)\big] \\ &= \int_0^\infty d\omega \iint d^2\mathbf{k}\,\mathbf{k}\,F_{\text{rad}}(k, \omega),\end{aligned} \tag{32}$$

whereas for the perpendicular direction, we note that the resulting expression for the emitted radiation in the far field,

$$\begin{aligned}p^{\perp}_{\text{rad}} = -\frac{1}{32\pi^4}\int_0^\infty d\omega \iint d^2\mathbf{k}\,\text{Re}[|\widetilde{E}^{\perp}_{\text{ind}}(\mathbf{k}, d, \omega)|^2 - \widetilde{\mathbf{B}}^{\parallel}_{\text{ind}}(\mathbf{k}, d, \omega)\cdot\widetilde{\mathbf{B}}^{\parallel *}_{\text{ind}}(\mathbf{k}, d, \omega) \\ - \big|\widetilde{E}^{\perp}_{\text{ind}}(\mathbf{k}, -d, \omega)\big|^2 + \widetilde{\mathbf{B}}^{\parallel}_{\text{ind}}(\mathbf{k}, -d, \omega)\cdot\widetilde{\mathbf{B}}^{\parallel *}_{\text{ind}}(\mathbf{k}, -d, \omega)],\end{aligned} \tag{33}$$

vanishes identically because the terms with $z = d$ are equal to the corresponding terms with $z = -d$, which appear with the opposite sign.

Referring to Eq. (30) for $j = x$ and y and to Eq. (32), we see that it is the Maxwell "shear stress" that gives rise to a momentum carried by the induced EM radiation in the far-field region, which compensates the "missing" momentum on all charges that was found in Eq. (29) to occur in the parallel direction. Therefore, the conservation of momentum in the parallel direction may be expressed as $\mathbf{p}^{\parallel}_{\text{ext}} + \mathbf{p}^{\parallel}_{\text{ohm}} + \mathbf{p}^{\parallel}_{\text{rad}} = \mathbf{0}$, whereas conservation of momentum in the perpendicular direction only includes charges in the system, giving $p^{\perp}_{\text{ext}} + p^{\perp}_{\text{ohm}} = 0$. Clearly, the overall momentum is conserved: $\mathbf{p}_{\text{ext}} + \mathbf{p}_{\text{ohm}} + \mathbf{p}_{\text{rad}} = \mathbf{0}$.

Finally, the somewhat unexpected difference in the joint densities for parallel and perpendicular momentum transfers to the sheet, appearing in Eqs. (25) and (28), may be verified by implementing a similar procedure, which involves integration of Eq. (18) over time, but for a volume V_0 defined by $d \to 0^+$, which envelops the conducting sheet tightly. In that case $\mathbf{p}_{\text{ext}} = \mathbf{0}$, so the total momentum imparted on charged particles is reduced to just those in the sheet, $\mathbf{p} = \mathbf{p}_{\text{ohm}}$, with its parallel and perpendicular components still given by the expressions in Eqs. (25) and (28), respectively. Let us next denote the momentum resulting from integrating the third term in Eq. (18) over time by $\mathbf{p}_{\text{str}}$ to indicate that it results from the flux of the Maxwell stress tensor through the planes $z = 0^{\pm}$. Decomposing it into parallel and perpendicular components, $\mathbf{p}_{\text{str}} = \mathbf{p}^{\parallel}_{\text{str}} + \hat{\mathbf{z}}\,p^{\perp}_{\text{str}}$, we find

$$\mathbf{p}^{\parallel}_{\text{str}} = -\int_0^\infty d\omega \iint d^2\mathbf{k}\,\mathbf{k}\,F_{\text{ohm}}(k, \omega), \tag{34}$$

and

$$p^{\perp}_{\text{str}} = -\int_0^\infty d\omega \iint d^2\mathbf{k}\,\frac{\omega}{v}\,F_{\text{ext}}(k, \omega), \tag{35}$$

so that, indeed, $\mathbf{p}^{\parallel}_{\text{ohm}} + \mathbf{p}^{\parallel}_{\text{str}} = \mathbf{0}$ and $p^{\perp}_{\text{ohm}} + p^{\perp}_{\text{str}} = 0$. By writing the conservation relation in the case of volume V_0 for all three components as $\mathbf{p}_{\text{ohm}} + \mathbf{p}_{\text{str}} = \mathbf{0}$, we generalize the well-known equivalence of using the distributed Lorentz force and the Maxwell stress tensor in calculations of radiation pressure on dielectric boundaries [67] to the case of incident charged particles upon 2D materials. In particular, the equality $p^{\perp}_{\text{ohm}} + p^{\perp}_{\text{str}} = 0$ demonstrates that using the definitions in Eqs. (26) and (27) to integrate the density of the Lorentz force "inside" a 2D material represented by a Dirac delta [66,68] is consistent with the flux of the Maxwell stress tensor through the adjacent planes, which is determined by the EM fields *outside* the 2D material.

III. CONCLUDING REMARKS

We have performed a detailed analysis of conservation relations for the electromagnetic energy and momentum during inelastic scattering of a fast charged particle, which passes through an isotropic conductive sheet under normal incidence without recoil. While verifying the energy conservation, we have shown that each subsystem, namely, the external charged particle, electrons in the sheet, and EM radiation in the far-field region, is characterized by a unique function of the in-plane wavevector and angular frequency, $F_{\text{L}}(\mathbf{k}, \omega)$ with $\text{L} = \text{ext}, \text{ohm}, \text{rad}$, respectively. Treating ω and $\mathbf{k}$ as "random" variables and the functions $F_{\text{L}}(\mathbf{k}, \omega)$ as joint probability densities [55–57], the energy change in each subsystem, W_{L}, is evaluated as the first moment of ω. When discussing the conservation of momentum, we have demonstrated that those same functions define the change in the momentum,

$\mathbf{p}_L$, in each subsystem as the first moment of the vector $(\mathbf{k}, \omega/v)$. It should be stressed that both the conservation of energy, $W_{ext} + W_{ohm} + W_{rad} = 0$, and conservation of momentum, $\mathbf{p}_{ext} + \mathbf{p}_{ohm} + \mathbf{p}_{rad} = \mathbf{0}$, are facilitated by a general relation between the joint densities, $F_{ext} = F_{ohm} + F_{rad}$ for all ω and $\mathbf{k}$.

It should be noted that, for the special case of a normal incidence upon an isotropic 2D material, all the net changes in the parallel momenta should vanish by symmetry, because all the functions F_L depend on $k = \|\mathbf{k}\|$. However, a probabilistic interpretation of those functions as being related to a double differential cross section (per atom) for inelastic scattering of the incident charged particle allows us to calculate the second moment of k from F_{ext} and obtain a standard deviation in the change of the parallel momentum of that particle, $\Delta p^{\parallel}_{ext}$. This can be then used to estimate the deflection angle (and hence the beam broadening) of that particle as $\Delta p^{\parallel}_{ext}/p_0$, where $p_0 = \gamma m v$ is its incident momentum with $\gamma = 1/\sqrt{1 - v^2/c^2}$ (see, e.g., Secs. 3.2.3 and 3.3.1.5 in Ref. [69]). Moreover, our theory allows one to further treat the densities F_{ohm} and F_{rad} as being related to two distinct channels of the inelastic scattering event and to express this result in terms of standard deviations in the changes of the parallel momenta due to Ohmic and radiative losses as $\Delta p^{\parallel}_{ext} = \sqrt{(\Delta p^{\parallel}_{ohm})^2 + (\Delta p^{\parallel}_{rad})^2}$, enabling one to assess relative contributions of the electronic excitations in the sheet and the emitted radiation to the total beam broadening.

It is interesting that, while all three subsystems participate in the conservation of momentum in the parallel direction with their respective joint densities, the net change in the momentum carried by the radiation in the perpendicular direction is zero identically. In other words, the momentum transfer in the perpendicular direction only occurs between the incident particle and the electrons in the sheet. However, the calculation of the momentum transfer to the sheet in the perpendicular direction by means of the Lorentz force presents a challenge because it requires values of the perpendicular electric field and tangential magnetic field on the sheet, while those fields experience jump discontinuities across that sheet, as a consequence of the standard electromagnetic boundary conditions. We have overcome that challenge by applying a prescription, put forward in the literature pertaining to nano-optics [64–66], whereby one assigns an *average* of the values of those fields on both sides of the sheet to be their respective value on the sheet. We have confirmed the validity of that prescription by performing an independent test of the momentum conservation relation using an infinitesimally thin volume that straddles the sheet, thereby making the momentum pertaining to the external charged particle vanish. We have indeed found that changes in both the parallel and perpendicular momenta of electrons in the sheet, evaluated by means of the Lorentz force, are exactly equal (with the opposite sign) to the corresponding momenta derived from the flux of the Maxwell stress tensor across the adjacent planes on both sides of that sheet. While we have demonstrated in this way an internal consistency in our treatment of the EM fields in the presence of a polarizable 2D material, it would be interesting to further study this problem in the context of the Abraham-Minkowski debate [22,23,27].

It should be mentioned that we assumed that a 2D material can only be polarized in the parallel directions, which may be conveniently characterized by an in-plane conductivity function $\sigma(k, \omega)$. An important aspect of the problem at hand arises when the material can be polarized in the perpendicular direction, which has been discussed in the literature and was found to present some conceptual challenges regarding the stability of a continuous modeling of such a material [70,71] and it revealed subtle points regarding the very definition of an out-of-plane dielectric function for a perpendicularly polarizable 2D material in the context of its *ab initio* calculations [72–74]. It appears that an emerging consensus as to how to most consistently describe the perpendicular polarizability of a 2D material is to use an out-of-plane polarizability function $\alpha(k, \omega)$ [72–74]. Accordingly, a future development of the present theory will include a generalization that will incorporate this aspect of the model for a fully polarizable sheet.

Our theory has a potential to shed more light on the mechanisms of plasmon launching in a 2D material by the impact of a fast charged particle. While we did not specify the form of the conductivity function describing the electron excitations in the sheet, the appearance of the (near-)zero values of the resulting effective in-plane dielectric function $\epsilon(\mathbf{k}, \omega)$ has a well-established link with the occurrence of a collective mode in a 2D material, such as PP [58,75]. In such a situation, the function $F_{ohm}(\mathbf{k}, \omega)$ would exhibit a Dirac-delta-like singularity that introduces strong correlation between the variables ω and $\mathbf{k}$ in accord with the underlying PP dispersion relation. It would be, therefore, interesting to explore in the future how the concept of the "energy velocity" [27,29,30] fits in the present theory and how the group velocity of a collective mode in the sheet affects the overall energy-momentum balance in the system.

Finally, while our main text deals with normal incidence of a charged particle upon a sheet described by a scalar longitudinal conductivity, all the necessary generalizations for a more realistic setting with oblique incidence on a 2D material described by a tensorial, momentum-dependent in-plane conductivity are outlined in the Appendix. It is also shown there that, besides the two separate conservation relations for energy and momentum of the entire system, there exist simple energy-momentum conservation relations for its subsystems that may be written as $W_{ext} = \mathbf{v} \cdot \mathbf{p}_{ext}$ and $W_{ohm} + W_{rad} = \mathbf{v} \cdot (\mathbf{p}_{ohm} + \mathbf{p}_{rad})$, which are controlled by the velocity $\mathbf{v}$ of an obliquely incident charged particle in the no-recoil approximation (see Fig. 1).

ACKNOWLEDGMENTS

Z.L.M. acknowledges financial support from the Natural Sciences and Engineering Research Council of Canada (Grant No. 2016-03689). The Argentinean team acknowledges financial support from CONICET (research project PIP11220170100353) and National University of Cuyo (research project 06/C550).

APPENDIX: GENERALIZATION TO OBLIQUE INCIDENCE AND NON-SCALAR MATERIAL RESPONSE

While the main text outlines our theory for the special case of normal incidence of an external charged particle upon

an isotropic 2D material described by a scalar conductivity function $\sigma(k,\omega)$, the expressions for joint densities can be generalized to the case of an oblique incidence of the particle upon a 2D material described by a momentum-dependent in-plane conductivity tensor $\overleftrightarrow{\sigma}(\mathbf{k},\omega)$ as follows [45]:

$$F_{\rm ext}(\mathbf{k},\omega)=\frac{1}{4\pi^3\omega}{\rm Re}[\widetilde{\mathbf{E}}^*_{{\rm ext}\parallel}(\mathbf{k},0,\omega)\cdot\overleftrightarrow{\sigma}(\mathbf{k},\omega)\cdot\widetilde{\mathbf{E}}_{\parallel}(\mathbf{k},0,\omega)], \tag{A1}$$

$$F_{\rm ohm}(\mathbf{k},\omega)=\frac{1}{4\pi^3\omega}{\rm Re}[\widetilde{\mathbf{E}}^*_{\parallel}(\mathbf{k},0,\omega)\cdot\overleftrightarrow{\sigma}(\mathbf{k},\omega)\cdot\widetilde{\mathbf{E}}_{\parallel}(\mathbf{k},0,\omega)], \tag{A2}$$

$$F_{\rm rad}(\mathbf{k},\omega)=\frac{-1}{4\pi^3\omega}{\rm Re}[\widetilde{\mathbf{E}}^*_{\parallel}(\mathbf{k},0,\omega)\cdot\overleftrightarrow{\sigma}^{\rm H}(\mathbf{k},\omega)\cdot\overleftrightarrow{G}_{\parallel}(\mathbf{k},\omega)\cdot\overleftrightarrow{\sigma}(\mathbf{k},\omega)\cdot\widetilde{\mathbf{E}}_{\parallel}(\mathbf{k},0,\omega)]. \tag{A3}$$

Here, $\widetilde{\mathbf{E}}_{\parallel}(\mathbf{k},0,\omega)=\overleftrightarrow{\epsilon}^{-1}(\mathbf{k},\omega)\cdot\widetilde{\mathbf{E}}_{{\rm ext}\parallel}(\mathbf{k},0,\omega)$ replaces the expression in Eq. (4), with the in-plane dielectric permittivity being replaced by the in-plane dielectric tensor $\overleftrightarrow{\epsilon}(\mathbf{k},\omega)=\overleftrightarrow{I}_{\parallel}-\overleftrightarrow{G}_{\parallel}(\mathbf{k},\omega)\cdot\overleftrightarrow{\sigma}(\mathbf{k},\omega)$, and $\overleftrightarrow{\epsilon}^{-1}$ being the inverse of $\overleftrightarrow{\epsilon}$, while the superscript H in Eq. (A3) represents the conjugate transpose (or Hermitian adjoint). Expressions for the in-plane part of the electric dyadic Green's function (Green's tensor), $\overleftrightarrow{G}_{\parallel}(\mathbf{k},\omega)$, and the in-plane component of the electric field due to the external charged particle, $\widetilde{\mathbf{E}}_{{\rm ext}\parallel}(\mathbf{k},0,\omega)$, can be readily deduced from Eqs. (3) and (6) of Ref. [45], respectively. The changes in energy and momentum in each subsystem for the case of oblique incidence should be calculated as the first moments of ω and the vector $(\mathbf{k},Q)$, with the joint densities given in Eqs. (A1), (A2), and (A3). Note that, for a particle moving with the velocity $\mathbf{v}=\mathbf{v}_{\parallel}+\hat{\mathbf{z}}\,v_{\perp}$, the perpendicular component of the momentum transfer is generalized to $Q=(\omega-\mathbf{k}\cdot\mathbf{v}_{\parallel})/v_{\perp}$, where $\mathbf{v}_{\parallel}$ and $v_{\perp}$ are the parallel and perpendicular components of the velocity (see Fig. 1). With the above generalizations, all the conservation relations that are discussed in the main text are perfectly satisfied in a general case.

It should be emphasized that the above formulas are completely general and are applicable to all kinds of 2D materials and incidence directions of the external charged particle under the no-recoil approximation. The only considerations that need to be taken into account are that the induced EM fields should be correctly identified for the problem at hand, and that calculations are simplified if the bases for the representation of the EM fields, the conductivity, and the Green's tensors are suitably chosen and consistent. For example, if the above formulas are applied to graphene using a nonlocal conductivity model that supports both the longitudinal and transverse responses, then it is convenient to describe the EM fields, the conductivity, and the Green's tensors in the basis of longitudinal, $\hat{\mathbf{k}}$, and transverse, $\hat{\mathbf{z}}\times\hat{\mathbf{k}}$, unit vectors. For such a case, those quantities are given by Eqs. (17) and (18), (8), and (3) in Ref. [45], respectively. Moreover, as another example, if the above formulas are applied to an anisotropic 2D material, such as doped phosphorene, then it is convenient to describe the EM fields, the conductivity, and the Green's tensors in a basis of the principal in-plane directions of that material, e.g., by orienting the unit vectors $\hat{\mathbf{x}}$ and $\hat{\mathbf{y}}$ along its armchair and zigzag directions. Such considerations will be explored in future work [76].

Finally, it is interesting to note that, besides the separate energy and momentum conservation relations for the entire system, $W_{\rm ext}+W_{\rm ohm}+W_{\rm rad}=0$ and $\mathbf{p}_{\rm ext}+\mathbf{p}_{\rm ohm}+\mathbf{p}_{\rm rad}=\mathbf{0}$, there also exist relations connecting changes in energy and momentum in each subsystem. For example, for the external particle, we find

$$\begin{aligned}W_{\rm ext}-\mathbf{v}\cdot\mathbf{p}_{\rm ext}&=-\int_0^\infty d\omega\,\omega\iint d^2\mathbf{k}\,F_{\rm ext}(\mathbf{k},\omega)\\&\quad+\mathbf{v}\cdot\int_0^\infty d\omega\iint d^2\mathbf{k}\,(\mathbf{k}+Q\hat{\mathbf{z}})\,F_{\rm ext}(\mathbf{k},\omega)\\&=-\int_0^\infty d\omega\,\omega\iint d^2\mathbf{k}\,F_{\rm ext}(\mathbf{k},\omega)\\&\quad\times[\omega-\mathbf{v}\cdot(\mathbf{k}+Q\hat{\mathbf{z}})]\\&=0,\end{aligned} \tag{A4}$$

on the grounds that $v_{\perp}Q=\omega-\mathbf{k}\cdot\mathbf{v}_{\parallel}$. This form of an energy-momentum conservation, $W_{\rm ext}=\mathbf{v}\cdot\mathbf{p}_{\rm ext}$, is exactly what is expected for a change in energy and momentum in the no-recoil approximation, $\Delta E=\mathbf{v}\cdot\Delta\mathbf{p}$, for an incident particle with the energy E_0 and momentum $\mathbf{p}_0$, undergoing an inelastic scattering, such that $|\Delta E|\ll E_0$ and $\|\Delta\mathbf{p}\|\ll\|\mathbf{p}_0\|$.

On the other hand, for the Ohmic energy and momentum, we may use Eqs. (11) and (25), as well as Eq. (28) generalized to $p^{\perp}_{\rm ohm}=\int_0^\infty d\omega\iint d^2\mathbf{k}\,Q\,F_{\rm ext}(\mathbf{k},\omega)$, to show that

$$\begin{aligned}W_{\rm ohm}-\mathbf{v}\cdot\mathbf{p}_{\rm ohm}&=\int_0^\infty d\omega\iint d^2\mathbf{k}\,(\omega-\mathbf{k}\cdot\mathbf{v}_{\parallel})\\&\quad\times[F_{\rm ohm}(\mathbf{k},\omega)-F_{\rm ext}(\mathbf{k},\omega)],\end{aligned} \tag{A5}$$

which does not vanish. Moreover, taking into account Eqs. (15) and (32) and noting that Eq. (33) still implies that $p^{\perp}_{\rm rad}=0$ for oblique incidence, we have

$$W_{\rm rad}-\mathbf{v}\cdot\mathbf{p}_{\rm rad}=\int_0^\infty d\omega\iint d^2\mathbf{k}\,(\omega-\mathbf{k}\cdot\mathbf{v}_{\parallel})\,F_{\rm rad}(\mathbf{k},\omega), \tag{A6}$$

which is also nonzero. However, recalling the general conservation relation established in this article, namely, $F_{\rm ext}(\mathbf{k},\omega)=F_{\rm ohm}(\mathbf{k},\omega)+F_{\rm rad}(\mathbf{k},\omega)$, and using it in the right-hand sides of Eqs. (A5) and (A6), we may conclude that $W_{\rm ohm}+W_{\rm rad}=\mathbf{v}\cdot(\mathbf{p}_{\rm ohm}+\mathbf{p}_{\rm rad})$, linking the changes in energy and momentum pertaining to the 2D material and the EM radiation via the velocity of the incident particle.

[1] Y. Wu, G. Li, and J. P. Camden, Chem. Rev. **118**, 2994 (2018).
[2] A. Polman, M. Kociak, and F. J. García de Abajo, Nat. Mater. **18**, 1158 (2019).
[3] T. Coenen, B. J. Brenny, E. J. Vesseur, and A. Polman, MRS Bull. **40**, 359 (2015).
[4] C. I. Osorio, T. Coenen, B. J. M. Brenny, A. Polman, and A. F. Koenderink, ACS Photonics **3**, 147 (2016).
[5] M. Stöger-Pollach, L. Kachtík, B. Miesenberger, and P. Retzl, Ultramicroscopy **173**, 31 (2017).
[6] S. Mignuzzi, M. Mota, T. Coenen, Y. Li, A. P. Mihai, P. K. Petrov, R. F. M. Oulton, S. A. Maier, and R. Sapienza, ACS Photonics **5**, 1381 (2018).
[7] T. Zhao, S. Gong, M. Hu, R. Zhong, D. Liu, X. Chen, P. Zhang, X. Wang, C. Zhang, P. Wu *et al.*, Sci. Rep. **5**, 16059 (2015).
[8] I. Kaminer, Y. T. Katan, H. Buljan, Y. Shen, O. Ilic, J. J. López, L. J. Wong, J. D. Joannopoulos, and M. Soljačić, Nat. Commun. **7**, ncomms11880 (2016).
[9] X. Lin, I. Kaminer, X. Shi, F. Gao, Z. Yang, Z. Gao, H. Buljan, J. D. Joannopoulos, M. Soljačić, H. Chen *et al.*, Sci. Adv. **3**, e1601192 (2017).
[10] X. Shi, X. Lin, I. Kaminer, F. Gao, Z. Yang, J. D. Joannopoulos, M. Soljačić, and B. Zhang, Nat. Phys. **14**, 1001 (2018).
[11] C. Roques-Carmes, S. E. Kooi, Y. Yang, A. Massuda, P. D. Keathley, A. Zaidi, Y. Yang, J. D. Joannopoulos, K. K. Berggren, I. Kaminer *et al.*, Nat. Commun. **10**, 3176 (2019).
[12] F. R. Prudencio and M. G. Silverinha, Plasmonics **16**, 19 (2021).
[13] A. Ciattoni, C. Conti, and A. Marini, Phys. Rev. Appl. **15**, 054016 (2021).
[14] K. Tantiwanichapan, J. DiMaria, S. N. Melo, and R. Paiella, Nanotechnology **24**, 375205 (2013).
[15] T. Zhan, D. Han, X. Hu, X. Liu, S.-T. Chui, and J. Zi, Phys. Rev. B **89**, 245434 (2014).
[16] S. Liu, C. Zhang, M. Hu, X. Chen, P. Zhang, S. Gong, T. Zhao, and R. Zhong, Appl. Phys. Lett. **104**, 201104 (2014).
[17] L. J. Wong, I. Kaminer, O. Ilic, J. D. Joannopoulos, and M. Soljačić, Nat. Photonics **10**, 46 (2015).
[18] T. Zhao, M. Hu, R. Zhong, S. Gong, C. Zhang, and S. Liu, Appl. Phys. Lett. **110**, 231102 (2017).
[19] K.-C. Zhang, X.-X. Chen, C.-J. Sheng, K. J. A. Ooi, L. K. Ang, and X.-S. Yuan, Opt. Express **25**, 20477 (2017).
[20] S. Gong, M. Hu, Z. Wu, H. Pan, H. Wang, K. Zhang, R. Zhong, J. Zhou, T. Zhao, D. Liu, *et al.*, Photonics Res. **7**, 1154 (2019).
[21] J. P. Gordon, Phys. Rev. A **8**, 14 (1973).
[22] S. M. Barnett, Phys. Rev. Lett. **104**, 070401 (2010).
[23] D. J. Griffiths, Am. J. Phys. **80**, 7 (2012).
[24] O. M. Marago, P. H. Jones, P. G. Gucciardi, G. Volpe, and A. C. Ferrari, Nat. Nanotechnol. **8**, 807 (2013).
[25] D. Gao, W. Ding, M. Nieto-Vesperinas, X. Ding, M. Rahman, T. Zhang, C. Lim, and C.-W. Qiu, Light Sci. Appl. **6**, e17039 (2017).
[26] D. G. Kotsifaki and S. N. Chormaic, Nanophotonics **8**, 1227 (2019).
[27] K. Y. Bliokh, A. Y. Bekshaev, and F. Nori, Phys. Rev. Lett. **119**, 073901 (2017).
[28] L.-F. Yang and K. J. Webb, Phys. Rev. B **103**, 245124 (2021).
[29] J. Nkoma, R. Loudon, and D. R. Tilley, J. Phys. C **7**, 3547 (1974).
[30] A. Moradi, *Electromagnetic Problems Involving Two-Dimensional Electron Gases in Planar Geometry* (Springer, Berlin, 2020).
[31] F. J. García de Abajo, Rev. Mod. Phys. **82**, 209 (2010).
[32] J. Barthel and L. J. Allen, Phys. Rev. B **104**, 104108 (2021).
[33] F. J. García de Abajo, Phys. Rev. B **70**, 115422 (2004).
[34] A. Reyes-Coronado, R. G. Barrera, P. E. Batson, P. M. Echenique, A. Rivacoba, and J. Aizpurua, Phys. Rev. B **82**, 235429 (2010).
[35] P. E. Batson, A. Reyes-Coronado, R. G. Barrera, A. Rivacoba, P. M. Echenique, and J. Aizpurua, Nano Lett. **11**, 3388 (2011).
[36] P. Batson, A. Reyes-Coronado, R. Barrera, A. Rivacoba, P. Echenique, and J. Aizpurua, Ultramicroscopy **123**, 50 (2012), Albert Victor Crewe memorial issue.
[37] A. Rivacoba and N. Zabala, New J. Phys. **16**, 073048 (2014).
[38] N. Zabala and A. Rivacoba, Nucl. Instrum. Methods Phys. Res. Sect. B **354**, 105 (2015).
[39] M. J. Lagos, A. Reyes-Coronado, A. Konecna, P. M. Echenique, J. Aizpurua, and P. E. Batson, Phys. Rev. B **93**, 205440 (2016).
[40] J. Castrejon-Figueroa, J. A. Castellanos-Reyes, C. Maciel-Escudero, A. Reyes-Coronado, and R. G. Barrera, Phys. Rev. B **103**, 155413 (2021).
[41] Z. L. Miskovic, S. Segui, J. L. Gervasoni, and N. R. Arista, Phys. Rev. B **94**, 125414 (2016).
[42] K. Akbari, Z. L. Miskovic, S. Segui, J. L. Gervasoni, and N. R. Arista, ACS Photonics **4**, 1980 (2017).
[43] K. Akbari, Z. L. Miskovic, S. Segui, J. L. Gervasoni, and N. R. Arista, Nanotechnology **29**, 225201 (2018).
[44] K. Akbari, S. Segui, J. L. Gervasoni, Z. L. Miskovic, and N. R. Arista, Appl. Surf. Sci. **446**, 191 (2018).
[45] K. Akbari, S. Segui, Z. L. Miskovic, J. L. Gervasoni, and N. R. Arista, Phys. Rev. B **98**, 195410 (2018).
[46] Z. L. Miskovic, K. Akbari, S. Segui, J. L. Gervasoni, and N. R. Arista, Nucl. Instrum. Methods Phys. Res. Sect. B **422**, 18 (2018).
[47] K. Lyon, D. J. Mowbray, and Z. L. Miskovic, Radiat. Eff. Defects Solids **173**, 8 (2018).
[48] K. Lyon, D. J. Mowbray, and Z. L. Miskovic, Ultramicroscopy **214**, 113012 (2020).
[49] T. Djordjevic, I. Radovic, V. Despoja, K. Lyon, D. Borka, and Z. L. Miskovic, Ultramicroscopy **184**, 134 (2018).
[50] D. Novko, M. Šunjić, and V. Despoja, Phys. Rev. B **93**, 125413 (2016).
[51] V. Despoja, D. Novko, K. Dekanić, M. Šunjić, and L. Marušić, Phys. Rev. B **87**, 075447 (2013).
[52] V. Despoja, T. Djordjevic, L. Karbunar, I. Radovic, and Z. L. Miskovic, Phys. Rev. B **96**, 075433 (2017).
[53] G. Argentero, A. Mittelberger, M. Reza Ahmadpour Monazam, Y. Cao, T. J. Pennycook, C. Mangler, C. Kramberger, J. Kotakoski, A. K. Geim, and J. C. Meyer, Nano Lett. **17**, 1409 (2017).
[54] K. Müller, F. F. Krause, A. Béché, M. Schowalter, V. Galioit, S. Löffler, J. Verbeeck, J. Zweck, P. Schattschneider, and A. Rosenauer, Nat. Commun. **5**, 5653 (2014).
[55] J. Lindhard, Mat. Fys. Medd. K. Dan. Vidensk. Selsk. **28**, 1 (1954).
[56] J. Moyal, London Edinburgh Dublin Philos. Mag. J. Sci. **46**, 263 (1955).
[57] R. H. Ritchie, Phys. Rev. **114**, 644 (1959).
[58] Y. V. Bludov, A. Ferreira, N. M. R. Peres, and M. I. Vasilevskiy, Int. J. Mod. Phys. B **27**, 1341001 (2013).
[59] E. J. C. Dias and F. J. García de Abajo, ACS Nano **13**, 5184 (2019).

[60] C. Maciel-Escudero, A. Konečná, R. Hillenbrand, and J. Aizpurua, Phys. Rev. B **102**, 115431 (2020).
[61] C. Ophus, Microsc. Microanal. **25**, 563 (2019).
[62] J. D. Jackson, *Classical Electrodynamics* (Wiley, New York, 1975).
[63] D. J. Griffiths, *Introduction to Electrodynamics Prentice Hall* (Prentice-Hall, Englewood Cliffs, NJ, 1999).
[64] E. Kuester, M. Mohamed, M. Piket-May, and C. Holloway, IEEE Trans. Antennas Propag. **51**, 2641 (2003).
[65] M. Mansuripur, Opt. Express **12**, 5375 (2004).
[66] J. L. Cheng, J. E. Sipe, N. Vermeulen, and C. Guo, J. Phys.: Photonics **1**, 015002 (2018).
[67] B. A. Kemp, T. M. Grzegorczyk, and J. A. Kong, Opt. Express **13**, 9280 (2005).
[68] D. Griffiths and S. Walborn, Am. J. Phys. **67**, 446 (1999).
[69] R. F. Egerton, *Electron Energy-Loss Spectroscopy in the Electron Microscope* (Springer, New York, 2011).
[70] G. Barton, New J. Phys. **15**, 063028 (2013).
[71] M. Bordag, Phys. Rev. D **89**, 125015 (2014).
[72] L. Matthes, O. Pulci, and F. Bechstedt, Phys. Rev. B **94**, 205408 (2016).
[73] J. F. Dobson, T. Gould, and S. Lebègue, Phys. Rev. B **93**, 165436 (2016).
[74] T. Tian, D. Scullion, D. Hughes, L. H. Li, C.-J. Shih, J. Coleman, M. Chhowalla, and E. J. G. Santos, Nano Lett. **20**, 841 (2020).
[75] F. H. L. Koppens, D. E. Chang, and F. J. García de Abajo, Nano Lett. **11**, 3370 (2011).
[76] K. Akbari and Z. L. Miskovic (unpublished).